Insights into the ClC-4 Transport Mechanism from Studies of Zn^{2+} Inhibition

Jeremiah D. Osteen and Joseph A. Mindell
Membrane Transport Biophysics Unit, Porter Neuroscience Research Center, National Institute of Neurological Disorders and Stroke, National Institutes of Health, Bethesda, Maryland 20892

ABSTRACT The CLC family of chloride channels and transporters is a functionally diverse group of proteins important in a wide range of physiological processes. ClC-4 and ClC-5 are localized to endosomes and seem to play roles in the acidification of these compartments. These proteins were recently shown to function as Cl^-/H^+ antiporters. However, relatively little is known about the detailed mechanism of CLC-mediated Cl^-/H^+ antiport, especially for mammalian isoforms. We attempted to identify molecular tools that might be useful in probing structure-function relationships in these proteins. Here, we record currents from human ClC-4 (hClC-4) expressed in *Xenopus* oocytes, and find that Zn^{2+} inhibits these currents, with an apparent affinity of ~50 μM. Although Cd^{2+} has a similar effect, Co^{2+} and Mn^{2+} do not inhibit hClC-4 currents. In contrast, the effect of Zn^{2+} on the ClC-0 channel, Zn^{2+}-mediated inhibition of hClC-4 is minimally voltage-dependent, suggesting an extracellular binding site for the ion. Nine candidate external residues were tested; only mutations of three consecutive histidine residues, located in a single extracellular loop, significantly reduced the effect of Zn^{2+}, with one of these making a larger contribution than the other two. An analogous tri-His sequence is absent from ClC-0, suggesting a fundamentally different inhibitory mechanism for the ion on hClC-4. Manipulations that alter transport properties of hClC-4, varying permeant ions as well as mutating the "gating glutamate", dramatically affect Zn^{2+} inhibition, suggesting the involvement of a heretofore unexplored part of the protein in the transport process.

INTRODUCTION

The CLCs represent a homologous group of Cl^- transport proteins that play important roles in many physiological as well as pathological processes. Though all known CLCs transport Cl^- across membranes, fundamental aspects of the transport mechanism vary dramatically between members. A striking example of this functional diversity is the observation that some CLCs function as chloride ion channels, whereas others are coupled proton/chloride antiporters.

ClC-3, -4, and -5 are members of a highly homologous CLC subfamily primarily found in intracellular organelles (1). ClC-5 has been demonstrated to contribute to endosomal acidification in kidney (2), with loss-of-function mutations leading to the defects of proximal tubule solute resorption known as Dent's disease in humans (3). Though ClC-4 has been suggested to play a similar role (4), details of its physiology and mechanism remain unclear. Though ionic currents through ClC-4 and ClC-5 were first observed a decade ago (5), only recently were both ClC-4 and -5 shown to be Cl^-/H^+ antiporters (6,7), as was ClC-7 (8). Given the high homology (≈77%) within the CLC 3/4/5 subfamily, ClC-3 likely functions in a similar manner, though this protein has recently been also proposed to function as a chloride channel (9). The observations that ClC-4 and -5 are antiporters rather than ion channels imply that these proteins operate by fundamentally different mechanisms than their channel cousins, like ClC-0 and ClC-1. These proteins are also relatively distantly related to the prototypical CLC transporter ClC-ec1, suggesting that they may also demonstrate significant functional divergence from the bacterial transporter, with differences in both voltage dependence and ion coupling (10). Thus, biophysical understanding of these transporters requires independent analysis of the CLC-3/4/5 subfamily.

Several properties of mammalian CLC antiporters make mechanistic analysis difficult. First, no high affinity inhibitors are known for these proteins. Such inhibitors serve as valuable tools for probing structure and function in transport proteins. Second, ClC-4 and -5 currents display an extreme outward rectification when heterologously expressed (5), making reversal potentials impossible to measure. Without access to this property, it is difficult to address permeation and ion coupling in these proteins. Thus, development of novel tools to investigate the mechanistic features of these proteins is essential. One set of tools that has been useful in previous studies of CLC structure and function are divalent metal ions.

Divalent cations are known to interact with many membrane proteins, including members of the CLC family. For example, Zn^{2+} has been shown to inhibit currents from the channel CLCs, ClC-0, -1, and -2 (11–13). Studies of Zn^{2+} inhibition in ClC-0 reveal that zinc inhibits currents by preferentially binding to and stabilizing the closed state of the

Submitted May 9, 2008, and accepted for publication July 23, 2008.

Address reprint requests to Joseph A. Mindell, Membrane Transport Biophysics Unit, Porter Neuroscience Research Center, National Institute of Neurological Disorders and Stroke, National Institutes of Health, 35 Convent Drive, Bldg. 35, MSC 3701, Bethesda, MD 20892. Tel.: 301-402-3473; Fax: 301-480-1693; E-mail: mindellj@ninds.nih.gov.

Jeremiah D. Osteen's present address is the Program in Cellular, Molecular, and Biophysical Studies, Columbia University, New York, NY 10027.

Editor: Eduardo Perozo.

0006-3495/08/11/4668/08 $2.00

doi: 10.1529/biophysj.108.137158

slow gate, one of the two gating mechanisms described in these channels (11). Lin et al. showed that this effect can be reduced by mutating a cysteine residue (C^{212}) that is vital for slow gating (14), which corresponds to the extracellular end of helix G in the ClC-ec1 structure (15). Recent evidence also suggests that native *Xenopus* oocyte Cl^- currents, proposed to represent xClC-5 currents (16), display sensitivity to Zn^{2+}.

Here we demonstrate that Zn^{2+} inhibits currents from human ClC-4 heterologously expressed in *Xenopus* oocytes, and that it operates with an action strikingly different from its effect on the ClC-0 channel. Zn^{2+} has a moderate apparent affinity and its interaction with hClC-4 is minimally voltage-dependent, indicating an extracellular binding site. Mutational analysis identifies three residues, distant from the site corresponding to C^{212} in ClC-0, which reduce the Zn^{2+} effect. Surprisingly, mutation of the ''gating glutamate'', which uncouples Cl^- and H^+ transport and is distant from the likely binding site, completely abolishes the effect of Zn^{2+}. Furthermore, the effects of Zn^{2+} vary with the identity of the permeant anion. These observations suggest conformational coupling between the Zn^{2+} binding site and the ion permeation pathway.

MATERIALS AND METHODS

An expressed sequence tag (GenBank accession No. AA282953), coding for a full-length human ClC-4 cDNA, was cloned into the pBluescript SK vector. Though our sequence differs from the original hClC-4 GenBank sequence (accession number X77197), it is identical to the updated sequence (accession number NM_001830). Mutations were made using the Quickchange site-directed mutagenesis kit (Stratagene, La Jolla, CA), and verified by the DNA sequencing facility National Institute of Neurological Disorders and Stroke. Each mutant was sequenced fully, to ensure the absence of undesired mutations. RNA was transcribed in vitro using the mMessage mMachine T3 RNA polymerase kit (Ambion, Austin, TX).

ClC-4 was expressed in *Xenopus* oocytes, and currents were measured using a two-electrode voltage clamp with an OC-725C oocyte amplifier (Warner Instrument, Hamden, CT), and digitized using a Digidata 1321A interface and pCLAMP 9 software (Axon Instruments, Foster City, CA). Glass electrodes were pulled to resistances between.3–1 MΩ. Bath clamp electrodes were connected to wells containing 3 M KCl, and these were connected to the recording bath by 3-M KCl/agar bridges. Recordings were performed at room temperature in ND96 solution (96 mM NaCl, 2 mM KCl, 1.8 mM $CaCl_2$, 1 mM $MgCl_2$, and 5 mM HEPES, pH 7.4), unless otherwise stated. Recording solutions were perfused into the chamber by gravity flow. Divalent cations were added to the ND96 solution as chloride salts at the desired concentration. For anion substitution experiments, 80 mM NaCl was replaced with 80 mM NaBr, $NaNO_3$, or NaI.

Two voltage protocols were used to explore properties of wild-type (WT) and mutant hClC-4. To monitor expression and determine current-voltage relations, families of current traces were elicited by stepping from a −35-mV holding potential to voltages between −50 mV and +90 mV, each followed by a short test pulse to −80 mV. To screen for effects from divalent cations, we used identical repeated depolarizations to +60 mV for 300 ms, starting from a holding potential of −40mV. For all experiments, multiple batches of oocytes were examined. An entire batch of oocytes was discarded if uninjected cells from that batch had significant anion currents. Zn^{2+} measurements were bracketed by measurements in the absence of Zn^{2+}, and discarded if the inhibition was irreversible; this only occurred with $[Zn^{2+}] >$ 10 mM, rendering experiments impracticable at these concentrations.

Dose-response data were fit with a Hill equation, $y = (I_{max} x^n / K_{0.5}^n + x^n)$, where I_{max} is the maximum inhibition, n is the Hill coefficient, and $K_{0.5}$ is the concentration for half-maximal inhibition. Significance tests utilize the Student's t-test. For all measurements, $N = 3$–10, and error bars indicate the mean ± SE. Error bars are not shown when they are smaller than the symbols. Structures were rendered using PyMOL (DeLano Scientific, Palo Alto, CA).

RESULTS

Though hClC-4 is primarily an endosomal protein not normally expressed on the cell surface, upon overexpression in *Xenopus* oocytes, a significant number of transporters populate the cell membrane and can mediate ionic currents. The currents we observe are similar to those previously described (Fig. 1 *A*) (5,17,18): they are very strongly outwardly rectifying, displaying little or no inward current. Upon depolarization, hClC-4 currents exhibit two phases of activation: a fast component, which is already complete by the end of the capacitive transient, as well as a slower activation, on a millisecond timescale, which can be clearly seen in the current traces at positive voltages (Fig. 1 *A*). The extremely strong rectification provides a useful estimate of the amount of leak in a given oocyte, and the rectification remained strong in all tested permeant anions. Since the leaks we observe are linear, any significant inward current reflects contamination of the heterologously expressed hClC-4 current. We did not observe strong outward rectifying currents similar to hClC-4 in any

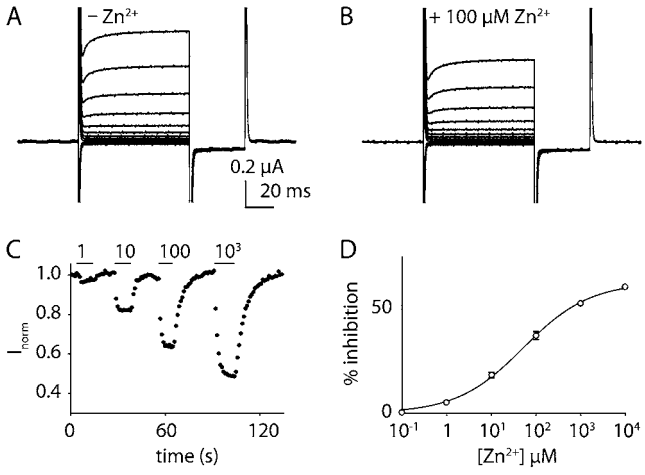

FIGURE 1 Zn^{2+} inhibition of hClC-4 currents. (*A* and *B*) hClC-4 currents measured in *Xenopus* oocytes with two-electrode voltage clamp in the absence (*A*) and presence (*B*) of 100 μM zinc. Voltage was held at −35 mV, pulsed from −50 to +90 in steps of 20 mV, and then to −80 mV before returning to holding potential. (*C*) Steady-state current responses to varying concentrations of extracellular zinc. Oocytes were held at −40 mV and pulsed repeatedly to +60 mV (*circles*) every 1 s. Solutions containing indicated concentrations (in μM) of $ZnCl_2$ were perfused into the chamber as indicated by bars; otherwise, chamber was perfused with ND96. Zinc inhibition was fully reversible in all cases. (*D*) Dose-response curve for ClC-4 at +60 mV, plotted on a logarithmic scale. For this and subsequent figures, error bars represent standard error of the mean ($N \geq 3$); when not shown, they are smaller than the symbols. Data are fitted with the Hill equation ($K_{0.5} = 52$ μM, $n = 0.58$, $I_{max} = 63\%$).

uninjected oocytes. This is consistent with the observations of Reyes et al. (16); they observed an outwardly rectifying endogenous oocyte current in some anions, but when Cl^- was the current carrier, the current was minimal. To further rule out contamination of measured currents by endogenous Cl^- channels, we recorded currents from uninjected oocytes in every batch of oocytes used in this study. The entire batch was discarded if substantial endogenous currents were present.

Extracellular Zn^{2+} inhibits outwardly rectifying hClC-4 currents (Fig. 1, *A* and *B*). Currents are elicited under constant perfusion; Zn^{2+} is introduced and washed out at a constant flow rate. Onset of inhibition takes place within the solution-exchange timescale for our perfusion system (seconds). Washout is slower, and is prolonged at higher Zn^{2+} concentrations (Fig. 1 *C*). Upon washout, currents return faithfully to their pre-Zn^{2+} levels (at $[Zn^{2+}]$ up to ~10 mM), demonstrating that Zn^{2+} inhibition is fully reversible in this concentration range. Zn^{2+} inhibition is dose-dependent, with maximal current reductions of ~60%, leaving a significant residual current. The residual current clearly reflects ion flux through hClC-4 since the full rectification of the current is maintained even at 1 mM Zn^{2+}: we see no evidence of increased leak. Zn^{2+} levels above 10 mM damage oocyte membranes, creating erratic responses to stimulation and making experiments at higher concentrations infeasible. The dose-response curve for Zn^{2+} is well fit by a Hill equation ($r^2 = 0.9986$), yielding an apparent affinity of ~50 μM, and a Hill coefficient of ~0.6. Cd^{2+} inhibits hClC-4 with similar dose-response properties compared with those of Zn^{2+}, whereas Mn^{2+} and Co^{2+} have no effect (Fig. 2, *A* and *B*) up to concentrations of 1 mM. The variable effects of different divalent metal ions reveal that the mechanism of inhibition by Zn^{2+} and Cd^{2+} cannot reflect simple electrostatic effect, since all four ions should screen surface charges on the protein to similar extents. Because the effects of Zn^{2+} and Cd^{2+} are so similar, we concentrated on the Zn^{2+} effect for further characterization.

We examined the voltage dependence of Zn^{2+} inhibition by comparing the effects of the ion at a series of positive potentials. Measurements at negative voltages could not be made because of the extreme rectification of the transporter. For a given oocyte, we measured the instantaneous and steady-state current at a series of voltages, then repeated these measurements in the presence of 100 μM Zn^{2+}, followed by a third set of measurements after removing Zn^{2+} to verify the reversibility of inhibition. Steady-state current-voltage relations in the presence and absence of 100 μM Zn^{2+} are shown for a typical oocyte in Fig. 3 *A*. Plotting the fractional inhibition as a function of voltage (Fig. 3 *B*) demonstrates that the Zn^{2+} effect is minimally dependent on membrane potential over the measurable range of voltages. Zn^{2+} has a similarly negligible effect on the voltage dependence of the instantaneous component of the hCLC-4 current (Fig. 3 *B*). Thus, Zn^{2+} is unlikely to traverse a significant fraction of the transmembrane voltage as it accesses its binding site on hClC-4: it probably binds at or near the extracellular surface of the transporter.

In ClC-0 and ClC-1, Zn^{2+} inhibition is strongly reduced by mutation of a conserved cysteine residue, C^{212} in ClC-0, which also plays a key role in the slow gating of this channel (14). However, there is no Cys residue in the analogous position on the hClC-4 gene, suggesting different coordinating residues, and perhaps a distinct mechanism of inhibition, for Zn^{2+} on hClC-4. Since Zn^{2+} usually binds proteins through interactions with cysteine and histidine moieties (19), we attempted to identify the Zn^{2+} binding site by focusing on these residues as candidate Zn^{2+} coordinating sites. Because of the minimal voltage dependence of Zn^{2+} inhibition, we examined residues predicted to lie on the extracellular side of the protein, as determined using the sequence alignment of hClC-4 and ClC-ec1 and a transmembrane topology derived from the ClC-ec1 crystal structure. Four histidine and five cysteine residues met these criteria (Fig. 4 *A*). We mutated each of these residues in turn, and screened the mutant transporters for changes in Zn^{2+} sensitivity that might reflect disruption of a metal binding site.

All mutants except C^{405S} express and produce currents similar to WT in the absence of Zn^{2+}. Mutations of three candidate residues affected Zn^{2+} inhibition: removing each of three sequential His residues, located on the extracellular

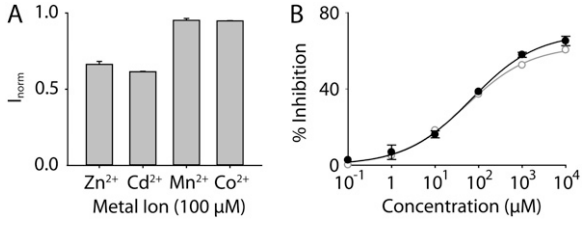

FIGURE 2 Effect of other divalent cations on hClC-4 currents. (*A*) Steady-state inhibition of currents by 100 μM extracellular Cd^{2+}, Co^{2+}, or Mn^{2+} at +50-mV holding potential, normalized to current in ND96. (*B*) Dose-response curve for extracellular Cd^{2+} (*solid symbols*, *solid line*), compared with dose-response curve for Zn^{2+} (*open symbols*, *gray line*; same data as shown in Fig. 1 *D*), both at +60 mV. Fit parameters for Cd^{2+}: $K_{0.5} = 68$ μM, $n = 0.58$, $I_{max} = 69\%$.

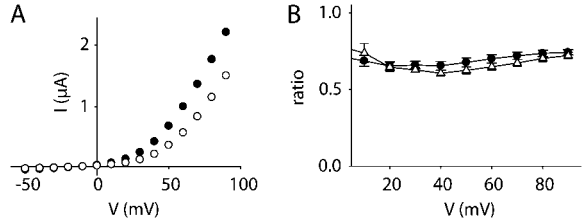

FIGURE 3 Voltage dependence of Zn^{2+} effect. (*A*) Representative I/V curves for steady-state hClC-4 currents plotted in absence (*solid circles*) or presence (*open circles*) of 100 μM Zn^{2+}. (*B*) Ratio of inhibited to uninhibited current in 100 μM Zn^{2+}, plotted as a function of voltage. Values are plotted for instantaneous (*open triangles*) and steady-state (*solid circles*) currents. Experimental points are connected with straight line segments.

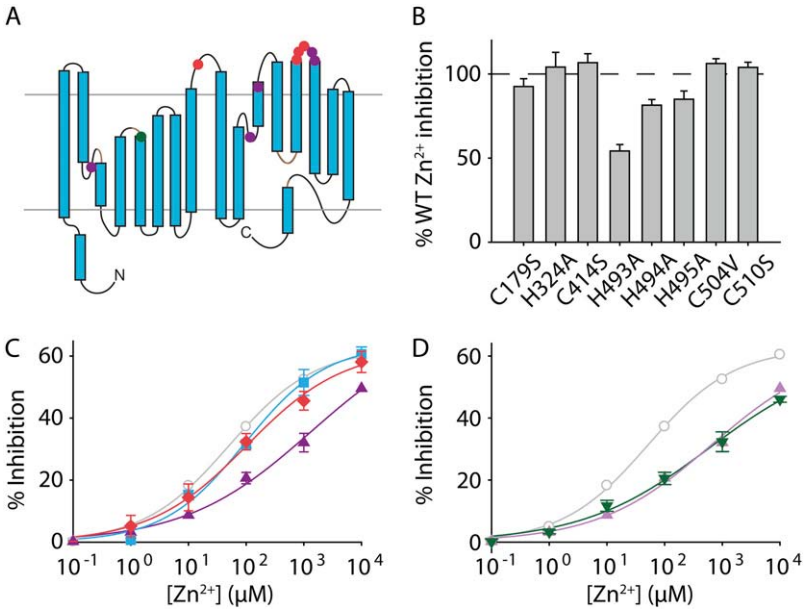

FIGURE 4 Mutation scan for Zn^{2+}-binding residues. (*A*) Extracellular and solvent-accessible cysteine and histidine residues in hClC-4, mapped onto ClC-ec1 topology. Candidate Zn^{2+} coordinating His (*red circles*) and Cys (*purple circles*) residues are shown. Green circle represents gating glutamate for reference. (*B*) Effect of 100 μM Zn^{2+} on mutants of candidate Zn^{2+}-coordination sites, expressed as percentage of WT inhibition by 100 μM Zn^{2+} at +60 mV. (*C*) Dose-response curves at +60 mV of single histidine mutants H^{493A} (*purple triangles* and *line*), H^{494A} (*blue squares* and *line*), and H^{495A} (*orange diamonds* and *line*); WT dose response is shown for comparison (*gray circles* and *line*). (*D*) Dose-response curve of double mutant H^{493A}/H^{495A} at +60 mV (*green triangles* and *line*), shown with those for H^{493A} (*purple*) and WT (*gray*) for comparison. Fit parameters: H^{493A} (constrained, see text), $K_{0.5} = 590$ μM, $n = 0.44$, $I_{max} = 63\%$; H^{494A}, $K_{0.5} = 95$ μM, $n = 0.52$, $I_{max} = 64\%$; H^{495A}, $K_{0.5} = 103$ μM, $n = 0.52$, $I_{max} = 62\%$; H^{493A}/H^{495A}, $K_{0.5} = 590$ μM, $n = 0.39$, $I_{max} = 61\%$.

loop between helices N and O (Fig. 4 *A*), produces a significant reduction in Zn^{2+} inhibition at 100 μM (Fig. 4 *B*). Comparing the dose-response curves of mutants with WT, we find that H^{494A} and H^{495A} each shifts the apparent affinity of the Zn^{2+} site by a small amount (Fig. 4 *C*; H^{494A}, $K_{0.5} = 95$ μM; H^{495A}, $K_{0.5} = 103$ μM), with saturation expected at the same level of inhibition as WT (63%). The mutation H^{493A} has a more dramatic effect (Fig. 4 *C*). Although we were unable to observe complete saturation of inhibition for H^{493A} in our range of usable Zn^{2+} concentrations, an unconstrained fit with a Hill equation yields a similar maximal inhibition to WT (71%), with the apparent affinity shifted by a factor of $\approx$26 ($K_{0.5} = 1.33$ mM). Alternatively, if we constrain the Hill equation fit to a maximal inhibition of 62.7%, i.e., the WT value, we find the affinity shifted ~12-fold ($K_{0.5} = 651$ μM). Regardless of the detailed, model-dependent parameters of the fit, it is clear that the H^{493A} mutation causes a shift of the Zn^{2+} dose-response corresponding to a considerable reduction in apparent affinity. Mutations of all remaining candidate extracellular Zn^{2+}-binding residues resulted in proteins displaying Zn^{2+} sensitivities similar to wild-type (Fig. 4 *B*).

The strong effect of mutating H^{493}, combined with the smaller effects of alterations at H^{494} and H^{495}, suggest that these residues might combine to form the Zn^{2+} binding site in hClC-4. If so, simultaneous mutations eliminating all three histidines might eliminate the site and the effect of Zn^{2+}. To test this hypothesis, we constructed proteins with all three histidines removed, or with each of the three possible pairs of His mutants. Of these, only H^{493A}/H^{495A} yields currents upon functional expression; it displays Zn^{2+} sensitivity almost identical to the single mutant H^{493A} (1.33 mM; Fig. 4 *D*, H^{493A}, *purple trace*; H^{493A}/H^{495A}, *green trace*), suggesting that H^{495} does not make a major contribution to residual Zn^{2+} binding in the H^{493A} mutant. Neither of the other combinations of double mutants (H^{493A}/H^{494A} or H^{494A}/H^{495A}) or the triple mutant (H^{493A}/H^{494A}/H^{495A}) expresses functionally in oocytes.

By analyzing an alignment between the protein sequence of hClC-4 and that of ClC-ec1, whose structure is known, we find that the residues apparently responsible for the Zn^{2+} binding site (H^{493}, H^{494}, and H^{495}) align with residues at the N-terminus of the extracellular loop connecting helix N to helix O in the ClC-ec1 structure (ClC-ec1, residues 381–383) (20). Interestingly, helix N projects into the core of the protein, and contributes main-chain hydrogen bonds to one of the bound Cl^- ions (at S_{cen}) and to the side chain of the gating glutamate (E^{148}; see Fig. 7). If the hClC-4 structure is similar to that of the *Escherichia coli* protein, then this observation suggests a mechanism of Zn^{2+} inhibition: Zn^{2+} binding could constrain a movement of helix N required for transport. This hypothesis predicts that there should be interactions between Cl^- binding and Zn^{2+} binding.

To test this hypothesis, we performed manipulations that could affect the occupancy of the Cl^- binding site. First, we mutated the hClC-4 residue corresponding to the ''gating glutamate'' in ClC-ec1 (21). In ClC-ec1 and ClC-5, neutralizing this conserved glutamate removes coupling between Cl^- and H^+ (6,7,22). As previously observed, the equivalent mutation in hClC-4 (E^{224A}) removes the rectification, and causes the protein to become a nearly linear Cl^- leak (Fig. 5 *A*) (5). Surprisingly, removing the hClC-4 gating glutamate also abolishes the inhibitory effect of Zn^{2+} at concentrations up to 1 mM. The 100-μM effect is shown in Fig. 5 *B* (*black open circles*); the linear conductance caused by the E^{224A} mutant (*solid circles*) is clearly different from the leak in uninjected oocytes (*gray circles*). This result is consistent with a model in which the chemical environment near the inner end of helix N projects to the relatively distant Zn^{2+} through movements of this helix.

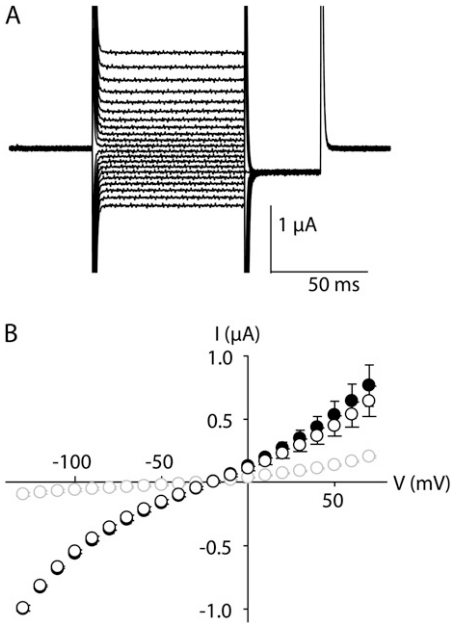

FIGURE 5 Gating glutamate mutant loses Zn^{2+} sensitivity. (*A*) Current traces from *Xenopus* oocytes express gating glutamate E^{224A} mutant. (*B*) Steady-state I/V curves for E^{224A} mutant in absence (*solid circles*) or presence (*open circles*) of 100 μM Zn^{2+}. For comparison, gray circles indicate currents measured in control uninjected oocytes.

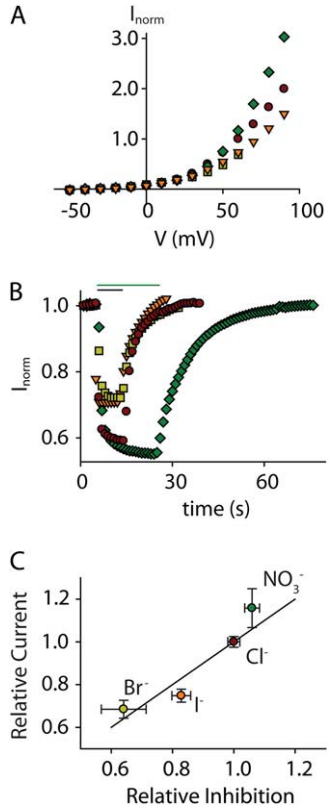

FIGURE 6 Interactions between anion permeation and Zn^{2+} inhibition. (*A*) I/V curves for WT ClC-4 in different external anions: Cl^- (*maroon circles*), I^- (*mustard squares*), Br^- (*orange downward triangles*), and NO_3^- (*green diamonds*). Data are normalized to current measured in Cl^- at +60 mV. (*B*) Inhibition by Zn^{2+} in different anions. A representative oocyte was held at −40 mV and pulsed repeatedly to +60 mV during application on 100 μM $ZnCl_2$ in presence of 96 mM external Cl^- (*maroon circles*); the oocyte was then perfused sequentially with solutions replacing 80 mM Cl^- with an equal concentration of I^- (*mustard squares*), Br^- (*orange downward triangles*), or NO_3^- (*green diamonds*). To allow comparison of degree of inhibition, currents were normalized to their value in each anion before addition of Zn^{2+}. In each case, they returned to baseline upon washout of Zn^{2+}. Black bar indicates time of Zn^{2+} exposure for Cl^-, Br^-, and I^-. Because of slower equilibration kinetics in NO_3^-, oocytes were exposed to Zn^{2+} for a longer time (*green bar*). (*C*) Correlation between current levels and extent of Zn^{2+} inhibition in varying anions. Currents measured at +60 mV in each anion are normalized to current in Cl^- at that voltage. Relative inhibition represents fractional inhibition measured for each anion, again normalized to the value for chloride.

We further tested this model by varying the identity of the permeant ion, another manipulation that could affect occupancy of the hClC-4 anion binding sites. Current levels for hClC-4 are known to vary with the permeant ion, with $NO_3^- > Cl^- > Br^- \sim I^-$ (5) (Fig. 6 *A*). When changing external anions, we sometimes observe an endogenous current similar to that described by Reyes et al. (16). However, it usually activates at stronger depolarizations than the heterologous current and is thus easily detected. Only when I^- was the current carrier did we observe consistent interfering endogenous currents. Because of these, we could not reliably measure hClC-4 currents +60 mV (note omission of these points in Fig. 6 *A*). We find that the degree of inhibition by 100 μM Zn^{2+} similarly varies as the permeant ion shifted; Zn^{2+} causes a greater inhibition when NO_3^- is the permeant ion than when Cl^- carries current (Fig. 6 *B*). (We verified that the inhibition reached a steady-state level by fitting the decay to a falling exponential plus a constant term; the constant term never differed from the data by more than 2.3%.) Indeed, the sequence of inhibitory effects is $NO_3^- > Cl^- > Br^- \sim I^-$. Plotting the fractional inhibition against the relative current in the different anions, we find an apparent correlation, with the data lying clustered around a line of slope 1 (Fig. 6 *C*). Ions that carry large currents through the transporter also exhibit large inhibition by Zn^{2+}, again consistent with the hypothesis that the N-helix mediates interactions between permeant ions and Zn^{2+} binding.

DISCUSSION

Our results agree with previous studies of hClC-4 that describe characteristic, strongly outwardly rectifying currents with a conduction sequence of $NO_3^- > Cl^- > Br^- \approx I^-$. Here we report that human ClC-4 is inhibited by Zn^{2+}, with a maximal inhibition of ~65% and an apparent affinity in the micromolar range. Although Zn^{2+} inhibition is characterized in other CLCs and in native outwardly rectifying chloride currents in *Xenopus* oocytes (16), to our knowledge, this is the first observation of a Zn^{2+} effect on a known CLC antiporter. Zn^{2+} inhibition is minimally voltage-dependent, suggesting that the metal ion acts near the extracellular face of the membrane.

Mutations of three extracellular histidine residues influence, but do not abolish this inhibition. Unexpectedly, manipulations that alter coupled ion transport, including mutation of the gating glutamate and variations of permeant anions, significantly influence the inhibitory effect of Zn^{2+}.

Zn^{2+} inhibits the CLC channels ClC-0, -1, and -2, presumably through a common mechanism. This inhibition was explored extensively for ClC-0, where Zn^{2+} inhibits by stabilizing the channel's slow gate in its closed state (11). A point mutation that abolishes slow gating significantly reduces the Zn^{2+} effect in ClC-0 (14). Though this mutation removes a cysteine, it remains unclear whether its effects result from weakened Zn^{2+} binding due to the removal of a coordinating residue, or simply from the disruption of the slow gating process in the context of preserved Zn^{2+} binding. Either way, we consider it unlikely that the binding site we identified in hClC-4 is analogous to a Zn^{2+} binding site in ClC-0, because the residues that influence hClC-4 Zn^{2+} binding site are not conserved in ClC-0, and are not replaced by other candidate Zn^{2+}-binding amino acids. Thus, it seems likely that Zn^{2+} inhibition in hClC-4 represents a distinct mechanism.

An unusual feature of hClC-4's inhibition by Zn^{2+} is its low Hill coefficient of ~0.6. Though the classical explanation for such a low Hill coefficient would be a negatively cooperative binding reaction, several other possibilities must also be considered. Negative cooperativity implies an interaction between multiple binding sites, where binding at one site decreases the binding affinity of an alternate site. This may be a possibility for hClC-4, given that the dimeric nature of the transporter implies the presence of at least two binding sites. However, studies of subunit interactions in ClC antiporters have not unearthed any significant intersubunit interactions as part of the transport process (10,23). An alternate explanation for a Hill coefficient <1 is the presence of electrostatic interactions. Such a situation might arise if, in addition to specific binding, Zn^{2+} is nonspecifically concentrated at the surface of the protein by its net negative surface charge. Increasing concentrations of Zn^{2+} would substantially screen the surface charge on the protein, and might interfere with binding of the ion at the specific site. This would effectively flatten out the dose response and result in a low Hill coefficient. A third possibility is that we are observing the effects of Zn^{2+} binding at several sites with distinct but similar affinities. Further experiments will be required to distinguish among these possibilities.

Of the known protein Zn^{2+} coordination sites, the majority consist of some combination of cysteine and histidine moieties (though the acidic residues aspartate and glutamate are also implicated in some Zn^{2+} coordination sites) (19). Since the apparent affinity of the Zn^{2+} site in hClC-4 is on the order of 50 μM, the Zn^{2+} binding site probably includes contributions from multiple amino acid side chains. Given the large reduction in Zn^{2+} affinity with mutation of H^{493}, it likely plays a major role in Zn^{2+} binding, whereas H^{494} and H^{495} may participate to a lesser degree. Though we were at first surprised to find that three sequential His residues affect Zn^{2+} binding, experience with binding of His-tagged proteins to metal-chelating columns suggests that such sequential residues can contribute to metal affinity (24). In addition, the small effects of the latter two may reflect a less intimate coordination than that of H^{493}. The double mutant H^{493A}/H^{495A} behaves very similarly to the single mutant H^{493A}, which is not unexpected, given that H^{493} seems to be the major residue involved in Zn^{2+} coordination. Because we could not express the triple mutant or the other two combinations of double mutants, we cannot conclusively rule out involvement by another, more distant, coordinating residue.

Although no structure is available for a mammalian CLC, the structure of an *E. coli* CLC homolog (ClC-ec1) has served as a useful framework for these proteins (25,26). Likely similar in overall structure to a CLC channel, the ClC-ec1 structure is probably an especially good model for hClC-4 transport since it functions as a Cl^-/H^+ exchanger. We used a sequence alignment of hClC-4 and ClC-ec1 to map the putative Zn^{2+} binding site onto the ClC-ec1 crystal structure, and find that the three histidine residues reside on an extracellular loop just above the N-helix. Though this loop is 12 amino acids longer in hClC-4, and there is no equivalent tri-His motif in ClC-ec1, our alignment places the histidines just after the top of the N-helix (Fig. 7 *A*). This helix projects to the extracellular side of the transporter from the core of the protein, where conserved residues at its amino terminus contribute to the coordination of Cl^- ions at the S_{cen} and S_{ext} binding sites (21) (Fig. 7 *B*). This area, adjacent to the ''gating glutamate'', is essential for H^+/Cl^- coupling.

We propose that Zn^{2+} binding near the top of the N-helix transmits a conformational change along the helix that can

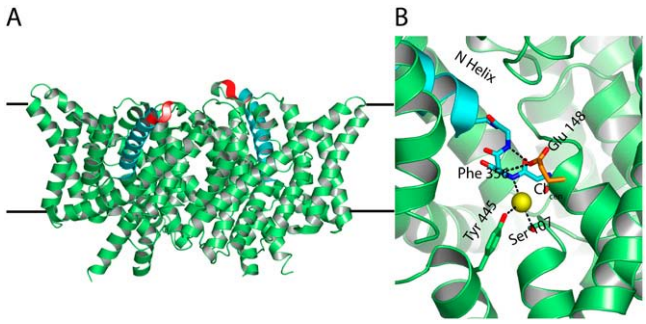

FIGURE 7 N-helix protrudes into core of permeation pathway and interacts with both Cl^- and H^+ binding sites. (*A*) Side-view of ClC-ec1. Mapped locations corresponding to H^{493}, H^{494}, and H^{495} of ClC-4 are highlighted in red. N-helix is shown in cyan. Approximate location of membrane boundary is indicated. (*B*) Bottom of N-helix (*cyan*) is shown, highlighting its interactions with central Cl^- binding site S_{cen} and gating glutamate (*orange*). Main-chain hydrogen bonds between N-helix residues and Glutamate^{148} and Cl^-_{cen} are shown as black dotted lines. Hydrogen bonds between Tyr^{445} and Cl^-_{cen}, and between Ser^{107} and Cl^-_{cen}, are also indicated. The central bound Cl^- (Cl^-_{cen}) is shown as a yellow sphere. Side chains of Tyr^{445}, Ser^{107}, and Glu^{148} are shown for reference. This view is from the dimer interface, with the four interfacial helices removed for clarity. Distances are in angstroms; structure is 1OTS from the Protein Data Bank (15).

couple interactions of the protein with permeant anions (or protons) to those between the protein and Zn^{2+}. This model comports well with our data showing that mutation of the gating glutamate has a profound effect on Zn^{2+} sensitivity, as the same conformational change could transmit between the protein core and the Zn^{2+} binding site. The observation that the Zn^{2+} effect is modulated by changing the permeant anion further supports this model, since we would expect, if Zn^{2+} indirectly interacts with anion binding through the N-helix, that the effect of this interaction would change based on the binding properties of the permeant anion. Alternatively, Zn^{2+} could interact not by affecting anion binding but through effects on the coupling between protons and anions. This would suggest an effect of Zn^{2+} not on the anion binding site, but on the coupling mechanism itself. Though the coupling ratios of protons with multiple halide ions have not been accurately measured for a mammalian CLC antiporter, coupling is qualitatively impaired when NO_3^- is the current carrier (10). This could explain some of our observations. Further experiments will be required to distinguish whether Zn^{2+} affects ion binding or proton coupling (or some other alternative), and to examine the nature and extent of the conformational change that mediates communication between the Zn^{2+} site and the transport pathway.

Zn^{2+} proves to be a valuable tool to probe structure and function of CLC transport, but may also represent a physiological role for hClC-4 in intracellular Zn^{2+} homeostasis. Although total cellular Zn^{2+} concentrations amount to 100–500 μM, unbound cytoplasmic concentrations of the ion are in the nanomolar range (27). Although much of the remaining cellular Zn^{2+} is bound to proteins as a cofactor in enzymatic reactions, Zn^{2+} may also be stored at much higher concentrations in vesicular compartments, including endosomes or late endosomes (28,29). These compartments contain specific Zn^{2+} transporters, and may serve to regulate cytoplasmic Zn^{2+} levels by sequestering excess Zn^{2+} in the endosomal lumen, especially in the face of toxic extracellular Zn^{2+} concentrations. Since the charge movement associated with Zn^{2+} transport would need to be neutralized, we speculate that hClC-4 could serve this role by moving a Cl^- counterion. In this light, perhaps the Zn^{2+} inhibition of hClC-4 reported here could play a role in the regulation of endosomal Zn^{2+} uptake.

The authors thank Kenton Swartz and his laboratory for assistance with oocyte recording and preparation, Dr. Swartz and Miguel Holmgren for critical reading of the manuscript, Dr. Emma Compton for help with PyMOL, and the other members of the Mindell Laboratory for helping us keep focused.

This work was funded by the National Institute of Neurological Disorders and Stroke Intramural Program.

REFERENCES

1. Gunther, W., A. Luchow, F. Cluzeaud, A. Vandewalle, and T. J. Jentsch. 1998. ClC-5, the chloride channel mutated in Dent's disease, colocalizes with the proton pump in endocytotically active kidney cells. *Proc. Natl. Acad. Sci. USA.* 95:8075–8080.
2. Piwon, N., W. Gunther, M. Schwake, M. R. Bosl, and T. J. Jentsch. 2000. ClC-5 Cl^--channel disruption impairs endocytosis in a mouse model for Dent's disease. *Nature.* 408:369–373.
3. Lloyd, S. E., S. H. Pearce, S. E. Fisher, K. Steinmeyer, B. Schwappach, S. J. Scheinman, B. Harding, A. Bolino, M. Devoto, P. Goodyer, S. P. Rigden, O. Wrong, T. J. Jentsch, I. W. Craig, and R. V. Thakker. 1996. A common molecular basis for three inherited kidney stone diseases. *Nature.* 379:445–449.
4. Mohammad-Panah, R., R. Harrison, S. Dhani, C. Ackerley, L. J. Huan, Y. Wang, and C. E. Bear. 2003. The chloride channel ClC-4 contributes to endosomal acidification and trafficking. *J. Biol. Chem.* 278: 29267–29277.
5. Friedrich, T., T. Breiderhoff, and T. J. Jentsch. 1999. Mutational analysis demonstrates that ClC-4 and ClC-5 directly mediate plasma membrane currents. *J. Biol. Chem.* 274:896–902.
6. Picollo, A., and M. Pusch. 2005. Chloride/proton antiporter activity of mammalian CLC proteins ClC-4 and ClC-5. *Nature.* 436:420–423.
7. Scheel, O., A. A. Zdebik, S. Lourdel, and T. J. Jentsch. 2005. Voltage-dependent electrogenic chloride/proton exchange by endosomal CLC proteins. *Nature.* 436:424–427.
8. Graves, A. R., P. K. Curran, C. L. Smith, and J. A. Mindell. 2008. The Cl^-/H^+ antiporter ClC-7 is the primary chloride permeation pathway in lysosomes. *Nature.*
9. Wang, X. Q., L. V. Deriy, S. Foss, P. Huang, F. S. Lamb, M. A. Kaetzel, V. Bindokas, J. D. Marks, and D. J. Nelson. 2006. CLC-3 channels modulate excitatory synaptic transmission in hippocampal neurons. *Neuron.* 52:321–333.
10. Zdebik, A. A., G. Zifarelli, E. Y. Bergsdorf, P. Soliani, O. Scheel, T. J. Jentsch, and M. Pusch. 2008. Determinants of anion-proton coupling in mammalian endosomal CLC proteins. *J. Biol. Chem.* 283:4219–4227.
11. Chen, T. Y. 1998. Extracellular zinc ion inhibits ClC-0 chloride channels by facilitating slow gating. *J. Gen. Physiol.* 112:715–726.
12. Kurz, L., S. Wagner, A. L. George Jr., and R. Rudel. 1997. Probing the major skeletal muscle chloride channel with Zn^{2+} and other sulfhydryl-reactive compounds. *Pflugers Arch.* 433:357–363.
13. Clark, S., S. E. Jordt, T. J. Jentsch, and A. Mathie. 1998. Characterization of the hyperpolarization-activated chloride current in dissociated rat sympathetic neurons. *J. Physiol.* 506:665–678.
14. Lin, Y. W., C. W. Lin, and T. Y. Chen. 1999. Elimination of the slow gating of ClC-0 chloride channel by a point mutation. *J. Gen. Physiol.* 114:1–12.
15. Dutzler, R. 2004. The structural basis of ClC chloride channel function. *Trends Neurosci.* 27:315–320.
16. Reyes, J. P., C. Y. Hernandez-Carballo, P. Perez-Cornejo, U. Meza, R. Espinosa-Tanguma, and J. Arreola. 2004. Novel outwardly rectifying anion conductance in *Xenopus* oocytes. *Pflugers Arch.* 449:271–277.
17. Hebeisen, S., H. Heidtmann, D. Cosmelli, C. Gonzalez, B. Poser, R. Latorre, O. Alvarez, and C. Fahlke. 2003. Anion permeation in human ClC-4 channels. *Biophys. J.* 84:2306–2318.
18. Vanoye, C. G., and A. L. George Jr. 2002. Functional characterization of recombinant human ClC-4 chloride channels in cultured mammalian cells. *J. Physiol.* 539:373–383.
19. Creighton, T. 1993. Proteins. Freeman, New York.
20. Dutzler, R., E. B. Campbell, M. Cadene, B. T. Chait, and R. MacKinnon. 2002. X-ray structure of a ClC chloride channel at 3.0 Å reveals the molecular basis of anion selectivity. *Nature.* 415:287–294.
21. Dutzler, R., E. B. Campbell, and R. MacKinnon. 2003. Gating the selectivity filter in ClC chloride channels. *Science.* 300:108–112.
22. Accardi, A., and C. Miller. 2004. Secondary active transport mediated by a prokaryotic homologue of ClC Cl^- channels. *Nature.* 427:803–807.
23. Nguitragool, W., and C. Miller. 2007. Inaugural article: CLC Cl /H+ transporters constrained by covalent cross-linking. *Proc. Natl. Acad. Sci. USA.* 104:20659–20665.

24. Hochuli, E., W. Bannwarth, H. Dobeli, R. Gentz, and D. Stuber. 1988. Genetic approach to facilitate purification of recombinant proteins with a novel metal chelate adsorbent. *Nat. Biotechnol.* 6:1321–1325.

25. Engh, A. M., and M. Maduke. 2005. Cysteine accessibility in ClC-0 supports conservation of the ClC intracellular vestibule. *J. Gen. Physiol.* 125:601–617.

26. Estevez, R., B. C. Schroeder, A. Accardi, T. J. Jentsch, and M. Pusch. 2003. Conservation of chloride channel structure revealed by an inhibitor binding site in ClC-1. *Neuron.* 38:47–59.

27. Eide, D. J. 2006. Zinc transporters and the cellular trafficking of zinc. *Biochim. Biophys. Acta.* 1763:711–722.

28. Palmiter, R. D., T. B. Cole, and S. D. Findley. 1996. ZnT-2, a mammalian protein that confers resistance to zinc by facilitating vesicular sequestration. *EMBO J.* 15:1784–1791.

29. Beyersmann, D., and H. Haase. 2001. Functions of zinc in signaling, proliferation and differentiation of mammalian cells. *Biometals.* 14: 331–341.